

Power-Efficiency Constraint for Biological Rotary Motor Driven by Chemical Gradient

Ruo-Xun Zhai¹ and Hui Dong^{1,*}

¹Graduate School of China Academy of Engineering Physics, Beijing, 100193, China

(Dated: May 7, 2024)

Biological motors, as counterpart of heat engines, are driven by a chemical gradient to output mechanical work and play critical roles in biological functions, such as the ATP synthesis. Its thermodynamic efficiency, along with power, are two vital criteria for evaluating the performance of these motors. In this letter, we investigate a model of a microscopic chemical engine and assess the constraint relation between power and efficiency for the cycle with finite operation time. Our model demonstrates a general constraint relation between power and efficiency, and predicts that the efficiency at maximum power in the large friction regime is half of the maximum quasi-static efficiency, i.e., $1/2$. These findings shall provide new direction to optimize the operation of microscopic biological motors.

Biological rotary motors, driven by ion concentration gradient, play important roles in living organisms to convert the free energy stored in the ionic gradient into mechanical energy to realize biological functions via thermodynamic cycles. For instance, ATP synthase with the F_0 - and F_1 -motor, is responsible for the synthesis of a major portion of ATP [1–15], which is the universal energy currency in living organisms. F_0 -motor, undergoing mechanical rotation driven by the chemical potential difference of positively charged ions (e.g. H^+ or Na^+), provides the primordial driving force in the ATP synthase.

The performance of the F_0 -motor is typically characterized by two quantities, thermodynamic efficiency and power. Thermodynamic efficiency is defined as the fraction of mechanical energy converted from the chemical free energy. And the power, measuring the mechanical work output per unit of time, is another crucial quantity in circumstances of changing energy request from the biological system. For instance, the instantaneous energy consumption power of a mouse can fluctuate from over 100kJ/day to around 20kJ/day [16]. This raises the question how the changing power affects the efficiency of the biological motors [17–19]. To address this question, the efficiency and power of such motors should be evaluated under the perspective of finite-time thermodynamics.

In this letter, we investigate the performance of a rotary motor resembling the F_0 -motor in the ATP synthase of *Propionigenium modestum* [5, 9]. The performance of the motor is tuned by varying both its angular velocity and its inside potential. Our analysis reveals the existence of a trade-off relation between power and efficiency for this motor. Such trade-off relation between power and efficiency is a fundamental characteristic of such finite-time motors.

Fig. 1 illustrates the current rotary motor, consisting of a rotor and a stator. The rotor has a ring structure made up of several c-subunits [6], represented by yellow blocks. These subunits feature negatively charged ionic binding sites, depicted by light blue and dark red circles.

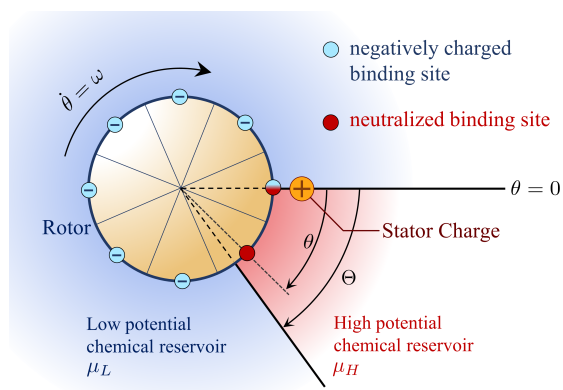


Figure 1. The rotary motor model consisting of a rotor and a stator. The rotor has a ring structure composed of multiple c-subunits, depicted by yellow blocks. Each subunit contains a negatively charged ionic binding site with the light blue representing the unbound state with negative charge and dark red as the neutralized bounded state. The rotation coordinate of the rotor is denoted as θ , where a clockwise rotation is defined as the positive direction. The stator interacts with the rotor through a fixed charge, represented by the large orange circle, located at $\theta = 0$. This charge provides an attractive inside potential $\Phi(\theta)$ for the negatively charged sites. The motor is in contact with both a high chemical potential (μ_H) reservoir (red shaded region) with the angular width Θ , and a low chemical potential (μ_L) reservoir (blue shaded region) simultaneously.

The charge of the sites can be neutralized by binding with one positively charged ion. The light blue and dark red colors on these sites correspond to the bound and unbound states respectively. The rotor's coordinate is denoted by θ , with clockwise rotation defined as the positive direction.

The rotor interacts with the stator via a fixed charge (the large orange circle), located at $\theta = 0$, which provides an attractive inside potential $\Phi(\theta)$ for the negatively charged sites. The exact form of the inside potential $\Phi(\theta)$ is obtained from the Coulomb interaction

* hdong@gscaep.ac.cn

between charges on the rotor and stator as

$$\Phi(\theta) = -\frac{\mathcal{E}}{\sqrt{\delta^2 + 2(1+\delta)(1-\cos\theta)}} + \Phi_0, \quad (1)$$

where $\delta = 0.1$ reflects the distance between the stator charge and the ring, and \mathcal{E} and Φ_0 are selected to ensure that $\Phi(\Theta) = -\Phi(0) = V/2$. Detailed discussion on the potential is shown in the Supplemental Materials.

The motor is in contact with two chemical reservoirs simultaneously: a high-potential chemical reservoir with chemical potential μ_H (the region $0 \leq \theta < \Theta$ with red shadow around the motor) and a low-potential chemical reservoir with chemical potential μ_L (the region $\Theta < \theta \leq 2\pi$ with blue shadow around the motor). Here, Θ is the angular width of the high potential reservoir. During the rotation, the binding sites alternate their contact between the high and low potential reservoirs.

When the motor reaches a steady cyclic rotation with a constant angular velocity ω , all the binding sites exhibit the same dynamics. To investigate the motor's performance, we examine the behavior of one specific binding site. The average binding number of negative charge for the binding site of interest is denoted by n with $0 \leq n \leq 1$. When the site is in equilibrium with a reservoir, the average binding number $n = n^{(0)}$ is determined by the reservoir's chemical potential $\mu(\theta)$ and the external inside potential $\Phi(\theta)$ as

$$n^{(0)}(\theta) = \frac{1}{1 + e^{\beta[E_b - \Phi(\theta) - \mu(\theta)]}}, \quad (2)$$

where $\beta = (k_B T)^{-1}$ is the inverse temperature of the reservoirs, and E_b is the energy of a neutralized site.

The ion exchange process between the binding site and the chemical reservoirs is described by a chemical reaction



The change rate of the average binding number n is proportional to the difference in particle number from equilibrium

$$\frac{dn}{dt} = -\left(n - n^{(0)}\right) / \tau_r, \quad (3)$$

where τ_r is the timescale of relaxation between the binding site and the reservoir. Here, we have assumed the same timescale τ_r for the relaxation in the two chemical reservoirs. Replacing the variable t in Eq. (3) with the angular coordinate $\theta = \theta_0 + \omega t$, we obtain the evolution equation of $n(\theta)$ as

$$\frac{dn}{d\theta} = -\frac{1}{\omega\tau_r} \left(n - n^{(0)}(\theta)\right), \quad (4)$$

with a periodic boundary condition $n(\theta) = n(\theta + 2\pi)$. The effect of finite operation time is characterized by the dimensionless coefficient $\omega\tau_r$.

The internal energy of the site is $U = nE_b + (1-n)\Phi(\theta)$ with its differential change $dU = [E_b - \Phi(\theta)]dn + (1-n)\Phi'(\theta)d\theta$. The first term is the energy change caused by the particle number relaxation into the reservoirs, and the second term represents the mechanical work $W_{\text{mech}} = \int_{-\pi}^{\pi} (1-n)\Phi'(\theta)d\theta$. Additionally, we include a linear dissipation $W_{\text{diss}} = 2\pi\gamma\omega$ with the linear friction coefficient γ to account for the resistance torque proportional to the angular velocity ω . And the net work output per cycle is

$$W_{\text{net}} = W_{\text{mech}} - W_{\text{diss}}. \quad (5)$$

The thermodynamic efficiency of the cycle is the ratio of the net work output W_{net} with respect to free energy decrease ΔF ,

$$\eta = \frac{W_{\text{net}}}{\Delta F}, \quad (6)$$

where the free energy decrease for the chemical reservoirs is $\Delta F = (\mu_H - \mu_L)\Delta n$ with $\Delta n = n(\Theta) - n(0)$ as the average number of particles transferred from the higher potential chemical reservoir to the lower one. And the average power is obtained as the average mechanical energy output rate per cycle

$$P = W_{\text{net}} / \tau_{\text{cycle}}, \quad (7)$$

where $\tau_{\text{cycle}} = 2\pi/\omega$ is the period of the rotation.

In the quasi-static limit with $\omega\tau_r \rightarrow 0$, the efficiency is an increasing function of the inside potential depth $V \equiv \Phi(\Theta) - \Phi(0)$ as

$$\eta^{(0)}(V) = \frac{k_B T}{\mu_H - \mu_L} \frac{\alpha_{\Theta H} \alpha_{0L}}{\alpha_{\Theta H} - \alpha_{0L}} \left(\ln \frac{\alpha_{0L}}{\alpha_{\Theta H}} - \ln \frac{\alpha_{\Theta L}}{\alpha_{\Theta H}} \right), \quad (8)$$

where $\alpha_{\Theta H} \equiv 1 + \exp(V/2 - E_b + \mu_H)$, $\alpha_{\Theta L} \equiv 1 + \exp(V/2 - E_b + \mu_L)$, $\alpha_{0H} \equiv 1 + \exp(-V/2 - E_b + \mu_H)$ and $\alpha_{0L} \equiv 1 + \exp(-V/2 - E_b + \mu_L)$. The detailed calculation is shown in the Supplemental Materials. The upper limit of quasi-static efficiency $\eta^{(0)}(V)$ is obtained as $\eta^{(0)} \rightarrow 1$ with $V \rightarrow \infty$, representing that all the free energy drawn from the reservoirs is converted into mechanical work. Nevertheless, such quasi-static cycles are impractical because the power output of a quasi-static cycle drops to 0, as the time span per cycle τ_{cycle} approaches infinity with $\omega \rightarrow 0$.

To acquire a finite output power, the motor rotates with a non-zero angular velocity ω . In Fig. 2, the curves show the average binding number $n(\theta)$ (in Fig. 2(a)) and the cumulative net work output $W_{\text{net}}(\theta) = \int_{-\pi}^{\theta} (dW_{\text{mech}} - dW_{\text{diss}})$ (in Fig. 2(b)) as functions of rotational coordinates θ for the range of $-\pi < \theta < \pi$. In the calculation, we set the width $\Theta = \pi/5$ and the dissipation coefficient $\gamma/(\tau_r k_B T) = 0.5$. The blue solid curve represents the quasi-static situation, and the green dashed and the red dash-dotted curve correspond to the angular velocity $\omega\tau_r = \pi/10$ and $\pi/3$ respectively. The red-shaded

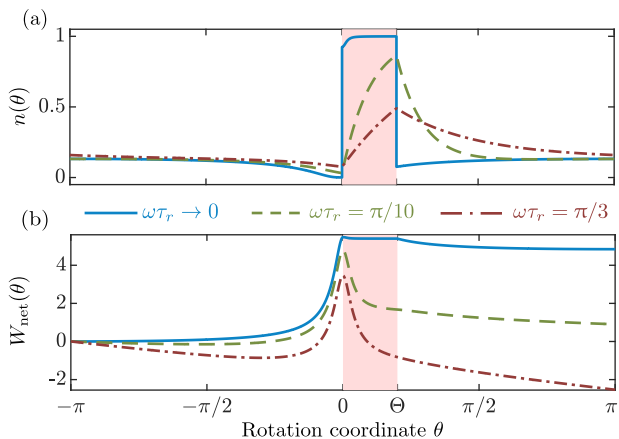


Figure 2. The average binding number n and the cumulative net work output W_{net} as functions of θ within finite operation time. (a) The average binding number $n(\theta)$. (b) The cumulative net work output $W_{\text{net}}(\theta)$. The horizontal coordinates are the same for the two subfigures. The parameters are fixed as follows: $V = 5k_B T$, $\mu_H = 10k_B T$, $\mu_L = 0$, $E_b = 5k_B T$, and $\gamma/(\tau_r k_B T) = 0.5$. The blue solid curve shows the quasi-static situation with $\omega \rightarrow 0$, and the finite time situations with $\omega\tau_r = \pi/10, \pi/3$ are shown in green dashed curve and red dash-dotted curve. The increasing of angular velocity causes the decreasing of total work output per cycle, which is reflected by the final value of the curves $W_{\text{net}}(\pi)$. The red shaded region ($0 \leq \theta < \Theta$) represents the system in contact with the high potential chemical reservoir.

areas illustrate the region where the binding site is in contact with the high-potential chemical reservoir. For the increasing angular velocity ω , the relaxation processes in the two chemical potential reservoirs become inadequate, and in turn result in the decrease of the output work as illustrated Fig. 2(b).

For fixed inside potential depth V , the output power depends on the angular velocity. To identify the optimal angular velocity ω that yields the maximum output power for a motor with a specified inside potential depth V , we examine the power and efficiency as functions of the angular velocity ω , as shown in Fig. 3(a) and (b) for different inside potential depths $V = 5k_B T$ (red squares) $10k_B T$ (purple diamonds) and $20k_B T$ (orange triangles). For fixed values of V , the curves show maximum output power at a optimal angular velocity ω , and the efficiency η decreases monotonically with respect to the angular velocity ω . The non-monotonic change of power and the monotonic decrease of efficiency highlight a constraint relation between the two quantities, and the possibility to find the optimal cycle with high efficiency for a certain power.

To determine the constraint relation, we search for the maximum efficiency achievable for a specified power output. The power and efficiency of 10^4 cycles are calculated with different combinations of angular velocity ω and inside potential depth V , and the results are plot-

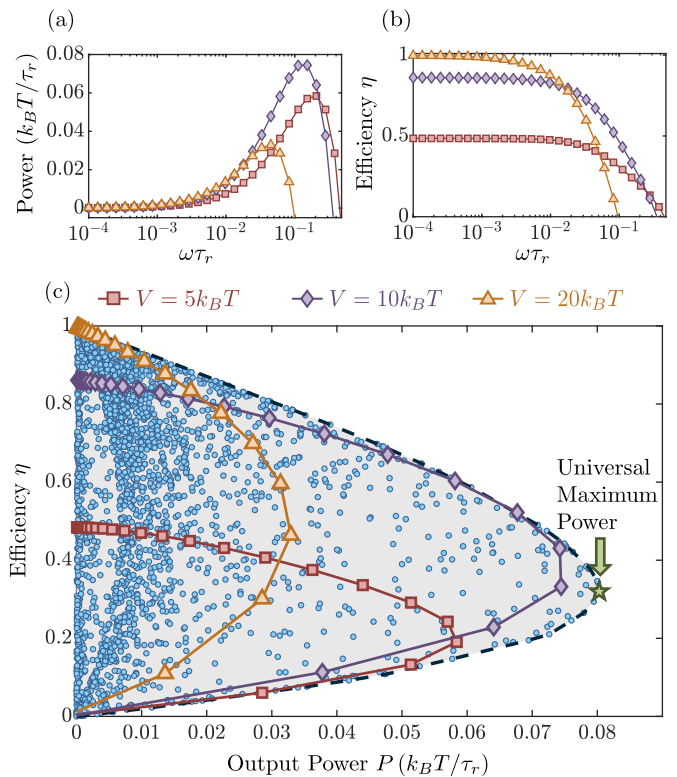


Figure 3. The constraint relation between the output power P and the efficiency. (a-b) The power and efficiency of finite-time cycles with respect to the angular velocity ω . The red squares, purple diamonds and orange triangles show the data with inside potential depth $V = 5, 10$, and $20k_B T$ respectively. (c) The constraint relation between power and efficiency. We randomly selected 10^4 different sets of ω and V , and evaluate the power and efficiency for each set. The blue circles represent data for different sets of ω and V . The gray shaded region enclosed by the black dashed line represents an envelope of the blue circles, illustrating the constraint relation between the power and efficiency. And the data for fixed V are shown with the same markers in (a-b), respectively. The green pentagram indicates the maximum power with $P^{(\text{max})} = 0.080k_B T/\tau_r$ and $\eta^{(\text{MP})} = 0.32$.

ted in Fig. 3(c). Each blue circle represents the power and efficiency of a combination of ω and V . The gray shaded region enclosed by the black dashed line represents an envelope of the blue circles, illustrating the constraint relation between the power and efficiency. The corresponding data in Fig. 3(a) and (b) with fixed inside potential depth V are plotted with the same markers in Fig. 3(c). The point with global maximum power is denoted by a green pentagram, featuring a maximum power $P^{(\text{max})} \approx 0.080k_B T/\tau_r$, and a corresponding efficiency, $\eta^{(\text{MP})} = 0.32$. The parameters at the maximum power are $V^{(\text{MP})} = 8.2k_B T$ and $\omega^{(\text{MP})}\tau_r = 0.054\pi$. Referring to Fig. 3(c), we can determine the optimal efficiency for any achievable power.

The efficiency at maximum power for the rotary motor depends on the friction coefficient γ . We present the

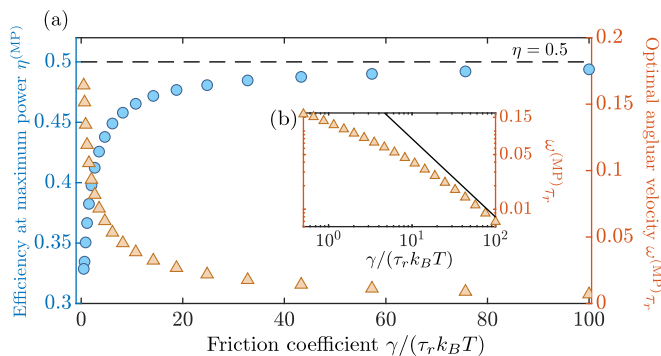


Figure 4. Efficiency at maximum power in large dissipation limit. (a) Dependence of the efficiency at maximum power and the corresponding optimal angular velocity on the friction coefficient γ . The blue circles indicate the efficiency at maximum power $\eta^{(\text{MP})}$ as a function of γ , and the orange triangles show the corresponding angular velocity $\omega^{(\text{MP})}\tau_r$. With the increase of friction coefficient, the optimal angular velocity $\omega^{(\text{MP})}\tau_r$ approaches 0 while the efficiency at maximum power approaches the theoretical bound $\eta = 1/2$. (b) The logarithmic plot of optimum angular velocity $\omega^{(\text{MP})}\tau_r$ with respect to γ . The black solid line represents the theoretical prediction in Eq. (9).

numerical results of the optimal angular velocity $\omega^{(\text{MP})}$ (orange triangles), and the efficiency at maximum power $\eta^{(\text{MP})}(\gamma)$ (blue circles) as functions of the friction coefficient γ in Fig. 4(a). In the large dissipation limit $\gamma \rightarrow \infty$, the optimal angular velocity $\omega^{(\text{MP})}$ approaches 0, and the efficiency at maximum power approaches 1/2, represented by the black dashed line. Such limit is proved in

the Supplemental materials. To the first order of $1/\gamma$, we obtain the optimal angular velocity and the corresponding efficiency as

$$\omega^{(\text{MP})} = (\mu_H - \mu_L)/4\pi\gamma + o(1/\gamma), \quad \eta^{(\text{MP})} = 1/2 + o(1/\gamma). \quad (9)$$

The theoretical results are in agreement with the numerical results in the limit with large γ . We note that the efficiency at maximum power has been examined in various models [18, 20–24] for chemical engines. The leading term with 1/2 for the efficiency at maximum power seems universal. Here, we provide an exact proof for such term in the rotary motor.

We would like to mention that much attention have been drawn to the thermodynamic properties of the microscopic chemical engines [17, 19, 25–35] with most of them concentrating on the F_1 motor and the interaction between the F_1 and F_0 parts. Yet the thermodynamic cycle for the F_0 portion is seldom explored, especially for its dynamic impact on power and efficiency. In this letter, we have evaluated the constraint relation between the power and efficiency of a biological rotary motor operating at a constant angular velocity, considering various parameters such as the angular velocity, the depth of the inside potential and the friction coefficient. The efficiency at maximum power approaches 1/2 in the limit with large dissipation coefficient. We anticipate that this research will inspire additional investigations into the thermodynamics of microscopic motors.

This work is supported by the Innovation Program for Quantum Science and Technology (Grant No. 2023ZD0300700), and the National Natural Science Foundation of China (Grant Nos. U2230203, U2330401, and 12088101).

-
- [1] P. Mitchell, *Nature* **191**, 144 (1961).
 [2] P. D. Boyer, *Annu. Rev. Biochem.* **66**, 717 (1997).
 [3] P. D. Boyer, *Angew. Chem. Int. Ed.* **37**, 2296 (1998).
 [4] T. Elston, H. Wang, and G. Oster, *Nature* **391**, 510 (1998).
 [5] P. Dimroth, H. Wang, M. Grabe, and G. Oster, *PNAS* **96**, 4924 (1999).
 [6] D. D. Hackney and F. Tamanoi, *The enzymes.*, 3rd ed. (Elsevier Academic Press, Amsterdam, 2004).
 [7] J. Xing, H. Wang, C. von Ballmoos, P. Dimroth, and G. Oster, *Biophys.* **87**, 2148 (2004).
 [8] W. Junge and N. Nelson, *Science* **308**, 642 (2005).
 [9] C. Von Ballmoos, A. Wiedenmann, and P. Dimroth, *Annu. Rev. Biochem.* **78**, 649 (2009).
 [10] W. Junge, H. Sialaff, and S. Engelbrecht, *Nature* **459**, 364 (2009).
 [11] R. Phillips, *Physical biology of the cell*, second edition ed. (Garland Science, London : New York, NY, 2013).
 [12] W. Junge and N. Nelson, *Annu. Rev. Biochem.* **84**, 631 (2015).
 [13] B. Chapman and D. Loiseau, *Royal Soc. Open Sci.* **3**, 150379 (2016).
 [14] K.-i. Okazaki and G. Hummer, *PNAS* **112**, 10720 (2015).
 [15] W. Kühlbrandt, *Annu. Rev. Biochem.* **88**, 515 (2019).
 [16] J. Speakman, *Front. Physiol.* **4** (2013).
 [17] S. Sieniutycz, *Int. J. Heat Mass Transf.* **51**, 5859 (2008).
 [18] H. Hooyberghs, B. Cleuren, A. Salazar, J. O. Indekeu, and C. Van den Broeck, *J. Chem. Phys.* **139**, 134111 (2013).
 [19] Y. Zhang, C. Huang, G. Lin, and J. Chen, *Physica A* **474**, 230 (2017).
 [20] L. Chen, F. Sun, C. Wu, and J. Yu, *Energy Convers. Manag.* **38**, 1841 (1997).
 [21] T. Schmiedl and U. Seifert, *EPL* **81**, 20003 (2007).
 [22] M. Esposito, K. Lindenberg, and C. Van den Broeck, *Phys. Rev. Lett.* **102**, 130602 (2009).
 [23] B. Gaveau, M. Moreau, and L. S. Schulman, *Phys. Rev. Lett.* **105**, 060601 (2010).
 [24] N. Golubeva and A. Imparato, *Phys. Rev. Lett.* **109**, 190602 (2012).
 [25] F. Jülicher, A. Ajdari, and J. Prost, *Rev. Mod. Phys.* **69**, 1269 (1997).
 [26] C. Bustamante, D. Keller, and G. Oster, *Acc. Chem. Res.* **34**, 412 (2001).

- [27] Y. Q. Gao, W. Yang, and M. Karplus, *Cell* **123**, 195 (2005).
- [28] W. R. Bauer and W. Nadler, *J. Chem. Phys.* **129** (2008), 10.1063/1.3026736.
- [29] U. Seifert, *Rep. Prog. Phys.* **75**, 126001 (2012).
- [30] K. K. Mandadapu, J. A. Nirody, R. M. Berry, and G. Oster, *PNAS* **112**, E4381 (2015).
- [31] M. R. Wilson, J. Solà, A. Carlone, S. M. Goldup, N. Lebrasseur, and D. A. Leigh, *Nature* **534**, 235 (2016).
- [32] G. Ai, P. Liu, and H. Ge, *Phys. Rev. E* **95**, 052413 (2017).
- [33] E. Lathouwers, J. N. E. Lucero, and D. A. Sivak, *J. Phys. Chem. Lett.* **11**, 5273 (2020).
- [34] E. Lathouwers and D. A. Sivak, *Phys. Rev. E* **105**, 024136 (2022).
- [35] M. P. Leighton and D. A. Sivak, *Phys. Rev. Lett.* **130**, 178401 (2023).

Supplemental Material for “Power-Efficiency Constraint for Biological Rotary Motor Driven by Chemical Gradient”

Ruo-Xun Zhai¹ and Hui Dong^{1, *}

¹Graduate School of China Academy of Engineering Physics, Beijing, 100193, China

(Dated: May 7, 2024)

This supplemental material provides detailed derivations and discussions related to the main text. In Section I, we determine the efficiency of a biological rotary motor operating in the quasi-static limit. In Section II, we derive the form of the inside potential used in the main text based on Coulomb’s law. In Section III, we discuss the condition for maximizing the output power in the limit of the dissipation coefficient γ approaching infinity.

MAXIMUM QUASI-STATIC EFFICIENCY

In this section, we derive the efficiency of the biological rotary motor in the quasi-static limit with $\omega \rightarrow 0$. During the infinitely slow rotation, the binding site is always in equilibrium with the reservoir, and the average binding number as a function of θ is $n^{(0)}(\theta) = (1 + e^{\beta(E_b - \Phi(\theta) - \mu(\theta))})^{-1}$, where $\mu(\theta) = \mu_H$ ($\mu(\theta) = \mu_L$) for $0 < \theta \leq \Theta$ ($\Theta < \theta \leq 2\pi$). The energy dissipated due to the friction W_{diss} is 0 in this quasi-static limit. The net work output of a cycle in the quasi-static limit is then obtained as

$$\begin{aligned} W_{\text{net}}^{(0)} &= - \int_0^{2\pi} (1 - n(\theta)) \Phi'(\theta) d\theta \\ &= k_B T \left(\ln \frac{1 + e^{\beta(\Phi(0) - E_b + \mu_L)}}{1 + e^{\beta(\Phi(0) - E_b + \mu_H)}} - \ln \frac{1 + e^{\beta(\Phi(\Theta) - E_b + \mu_L)}}{1 + e^{\beta(\Phi(\Theta) - E_b + \mu_H)}} \right). \end{aligned} \quad (\text{S1})$$

We conclude that the quasi-static work is determined by the values of $\Phi(\theta)$ at the edges of the channel, i.e., $\Phi(0)$ and $\Phi(\Theta)$.

The number of particles transferred in a quasi-static cycle is

$$\Delta n^{(0)} = \frac{1}{1 + e^{-\beta(\Phi(\Theta) - E_b + \mu_H)}} - \frac{1}{1 + e^{-\beta(\Phi(0) - E_b + \mu_L)}}. \quad (\text{S2})$$

From Equations (S1) and (S2), the quasi-static efficiency is obtained as

$$\begin{aligned} \eta &= \frac{W_{\text{net}}^{(0)}}{(\mu_H - \mu_L) \Delta n^{(0)}} = \frac{k_B T}{\mu_H - \mu_L} \times \frac{[1 + e^{\beta(\Phi(\Theta) - E_b + \mu_H)}] [1 + e^{\beta(\Phi(0) - E_b + \mu_L)}]}{e^{\beta(\Phi(\Theta) - E_b + \mu_H)} - e^{\beta(\Phi(0) - E_b + \mu_L)}} \\ &\quad \times \left(\ln \frac{1 + e^{\beta(\Phi(0) - E_b + \mu_L)}}{1 + e^{\beta(\Phi(0) - E_b + \mu_H)}} - \ln \frac{1 + e^{\beta(\Phi(\Theta) - E_b + \mu_L)}}{1 + e^{\beta(\Phi(\Theta) - E_b + \mu_H)}} \right). \end{aligned} \quad (\text{S3})$$

In Fig. S1(a), we evaluate the quasi-static efficiency as a function of $\Phi(\Theta)$ and $\Phi(0)$, where the relevant parameters are chosen as $\mu_H - E_b = 5k_B T$, and $\mu_L - E_b = -5k_B T$. For the case $\Phi(\Theta) \rightarrow \infty$ and $\Phi(0) \rightarrow -\infty$, the efficiency approaches the upper bound of 100%.

As shown in Fig. S1(a), for fixed depth of the inside potential $V \equiv \Phi(\Theta) - \Phi(0)$, the maximum quasi-static efficiency is reached with $\Phi(\theta) = -\Phi(0) = V/2$. The quasi-static efficiency $\eta^{(0)}$ as a function of V is written as

$$\begin{aligned} \eta(V) &= \frac{k_B T}{\mu_H - \mu_L} \times \frac{[1 + e^{\beta(V/2 - E_b + \mu_H)}] [1 + e^{\beta(-V/2 - E_b + \mu_L)}]}{e^{\beta(V/2 - E_b + \mu_H)} - e^{\beta(-V/2 - E_b + \mu_L)}} \\ &\quad \times \left(\ln \frac{1 + e^{\beta(-V/2 - E_b + \mu_L)}}{1 + e^{\beta(-V/2 - E_b + \mu_H)}} - \ln \frac{1 + e^{\beta(V/2 - E_b + \mu_L)}}{1 + e^{\beta(V/2 - E_b + \mu_H)}} \right). \end{aligned}$$

This function is illustrated in Fig. S1(b). As V increases, the quasi-static efficiency approaches an upper limit of 1.

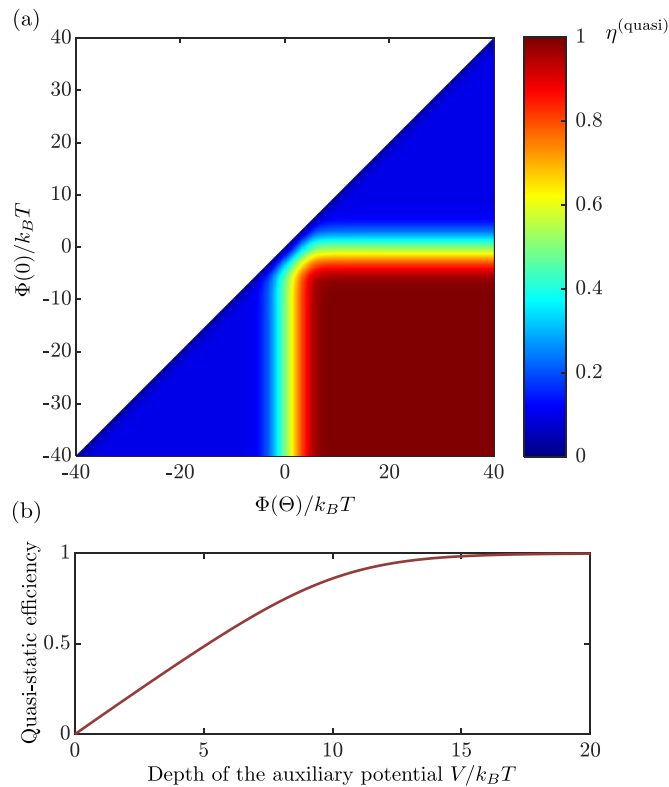


Figure S1. Quasi-static efficiency of biological rotary motor. (a) Quasi-static efficiency as a function of the value of inside potential $\Phi(\Theta)$ and $\Phi(0)$. The efficiency approaches the upper bound 100% when $\Phi(\Theta) \rightarrow \infty$ and $\Phi(0) \rightarrow -\infty$. Notably, for fixed depth $V \equiv \Phi(\Theta) - \Phi(0)$, the maximum quasi-static efficiency is reached with $\Phi(\theta) = -\Phi(0) = V/2$. (b) The efficiency for quasi-static cycles is shown as a function of the depth V . As V increases, the efficiency approaches its upper limit.

FORM OF THE INSIDE POTENTIAL

In this section, we derive the form of inside potential $\Phi(\theta)$ induced by the Coulomb interaction between the stator charge and the binding site. In Figure. S2, we denote the radius of rotor by R , and the distance between the stator charge and the center of the rotor by $(1 + \delta)R$. The distance between the binding site and the stator charge with respect to the rotation coordinate θ is acquired as $r = R\sqrt{\delta^2 + 2(1 - \cos\theta)\delta + 2(1 - \cos\theta)}$. The potential energy of the Coulomb interaction between the stator charge and the unbounded binding site is

$$\Phi(\theta) = -\frac{\mathcal{E}}{r} + \Phi_0. \quad (\text{S4})$$

Where Φ_0 defines the potential energy of infinity, and $\mathcal{E} \equiv q_1 q_2 / (4\pi\epsilon)$ with q_1, q_2 the charge for the binding site and stator charge, ϵ the permittivity of the medium. In the main text, we choose $\delta = 0.1$, and the parameters \mathcal{E} and Φ_0 are determined by the equations $\Phi(0) = -V/2$ and $\Phi(\Theta) = V/2$.

The plot of attractive inside potential $\Phi(\theta)$ is illustrated in Fig. S3 for $V = 5k_B T$. The red shaded region ($0 \leq \theta < \Theta$) represents the system in contact with the high potential chemical reservoir.

EFFICIENCY AT MAXIMUM POWER FOR LARGE DISSIPATION

In this section, we maximize the output power under the assumption of large dissipation $\gamma \rightarrow \infty$. For such case, the angular velocity should be small, i.e., $\omega\tau_r \ll 1$ to ensure positive power output. Therefore, we treat $\omega\tau_r$ as a

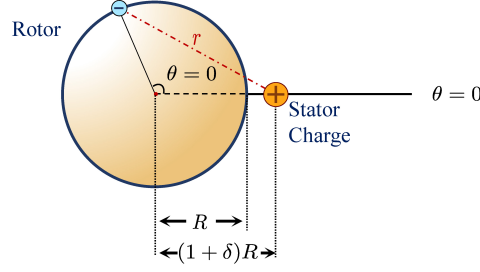


Figure S2. A sketch of the structure of the microscopic rotor. The radius of the rotor is denoted by R , and the distance between the center of the rotor and the stator is $(1 + \delta)R$. Together with Coulomb's law, we obtain the form of inside potential as Eq. (S4).

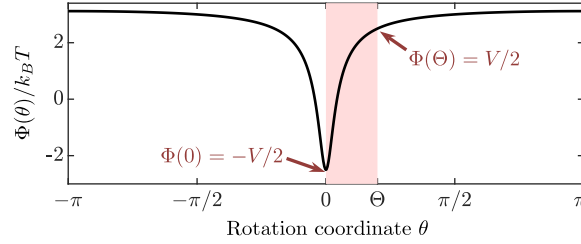


Figure S3. The inside potential Φ as a function of the angular position θ . The potential $\Phi(\theta)$ is induced by the Coulomb interaction with a minimum at $\theta = 0$. We set $\Phi(0) = -V/2$ and $\Phi(\Theta) = V/2$. In the plot, we have used the parameters with the depth of the inside potential as $V = 5k_B T$ and $\Theta = \pi/5$.

perturbation parameter and expand the solution of Eq. (4) in the main text to the first order of $\omega\tau_r$ as

$$n(\theta) = \begin{cases} n^{(0)}(\theta, \mu_H) - \omega\tau_r \frac{d}{d\theta} n^{(0)}(\theta, \mu_H), & 0 < \theta \leq \Theta, \\ n^{(0)}(\theta, \mu_L) - \omega\tau_r \frac{d}{d\theta} n^{(0)}(\theta, \mu_L), & \Theta < \theta \leq 2\pi. \end{cases} \quad (\text{S5})$$

The analytical expression for the mechanical work is given by $W_{\text{mech}} = -\int_0^{2\pi} n(\theta)\Phi'(\theta)d\theta = W^{(0)} - \omega\tau_r W^{(1)}$. Here, $W^{(0)}$ represents the quasi-static work as shown in Eq. (S1), and $W^{(1)}$ is an integral defined by

$$W^{(1)} = -\beta \int_0^{\Theta} \frac{e^{\beta(E_b - \Phi(\theta) - \mu_H)}}{[1 + e^{\beta(E_b - \Phi(\theta) - \mu_H)}]^2} [\Phi'(\theta)]^2 d\theta - \beta \int_{\Theta}^{2\pi} \frac{e^{\beta(E_b - \Phi(\theta) - \mu_L)}}{[1 + e^{\beta(E_b - \Phi(\theta) - \mu_L)}]^2} [\Phi'(\theta)]^2 d\theta.$$

Meanwhile, the particle number transferred during the finite time process is given by $\Delta n = \Delta n^{(0)} - \omega\tau_r \Delta n^{(1)}$, where

$$\Delta n^{(1)} = \frac{e^{\beta(E_b - \Phi(\Theta) - \mu_H)}}{[1 + e^{\beta(E_b - \Phi(\Theta) - \mu_H)}]^2} \Phi'(\Theta).$$

Taking the friction into account, we get $W_{\text{net}} = W^{(0)} - \omega(\tau_r W^{(1)} + 2\pi\gamma)$. The corresponding output power is $P(\omega, V) = \omega W^{(0)} - \omega^2(\tau_r W^{(1)} + 2\pi\gamma)$. To ensure $P > 0$, there is $0 < \omega\tau_r < W^{(0)}/(W^{(1)} + 2\pi\gamma/\tau_r)$. With $\gamma \rightarrow \infty$, we have $\omega\tau_r \rightarrow 0$, which is in agreement with the assumption that $\omega\tau_r$ being the perturbation parameter.

To maximize the output power of the cycle, we firstly optimize the angular velocity ω for fixed inside potential depth V . The maximum of P with respect to ω is reached as

$$P^{(\text{max})}(V) = \max_{\omega} (P(\omega, V)) = \left[W^{(0)} \right]^2 / (4\tau_r W^{(1)} + 2\pi\gamma), \quad (\text{S6})$$

with $\omega^{(\text{MP})}(V) = W^{(0)}/(2\tau_r W^{(1)} + 4\pi\gamma)$. Thus, the efficiency at this optimal angular velocity is

$$\eta^{(\text{MP})}(V) = \frac{W^{(0)} - \omega^{(\text{MP})}(V)(\tau_r W^{(1)} + 2\pi\gamma)}{(\mu_H - \mu_L) (\Delta n^{(0)} - \omega^{(\text{MP})}(V)\tau_r \Delta n^{(1)})} = \frac{W^{(0)}/2}{(\mu_H - \mu_L) (\Delta n^{(0)} - W^{(0)}\tau_r \Delta n^{(1)}/(2\tau_r W^{(1)} + 4\pi\gamma))}$$

With the situation that $\gamma \rightarrow \infty$, we keep the quantities to the first order of $1/\gamma$

$$P^{(\max)}(V) \approx \left[W^{(0)} \right]^2 / 2\pi\gamma, \quad \omega^{(\text{MP})}(V) \approx W^{(0)} / 4\pi\gamma. \quad (\text{S7})$$

And

$$\eta^{(\text{MP})}(V) \approx \frac{W^{(0)}(V)/2}{(\mu_H - \mu_L)\Delta n^{(0)}(V)} \left(1 + \frac{\Delta n^{(1)}(V)}{4\pi\Delta n^{(0)}(V)} \frac{W^{(0)}\tau_r}{\gamma} \right).$$

Then we optimize $P^{(\max)}(V)$ with respect to V . From Eq. (S7), the maximum of $P^{(\max)}(V)$ is achieved at the maximum of $W^{(0)}(V)$. By setting $\Phi(\theta) = -\Phi(0) = V/2$, the quasi-static work in Eq. (S1) is rewritten as a function of V as

$$W^{(0)}(V) = k_B T \left(\ln \frac{1 + e^{\beta(-V/2 - E_b + \mu_L)}}{1 + e^{\beta(-V/2 - E_b + \mu_H)}} - \ln \frac{1 + e^{\beta(V/2 - E_b + \mu_L)}}{1 + e^{\beta(V/2 - E_b + \mu_H)}} \right). \quad (\text{S8})$$

Whose upper limit is achieved only when $V \rightarrow \infty$ as $W_{\max}^{(0)} = \mu_H - \mu_L$. Thus, when $V \rightarrow \infty$, the power also achieve it's universal maximum as

$$P_{\max} = \left[W_{\max}^{(0)} \right]^2 / 2\pi\gamma = (\mu_H - \mu_L)^2 / 2\pi\gamma.$$

The efficiency at this maximum power is obtained as

$$\eta^{(\text{MP})} \rightarrow \frac{1}{2} + \text{O}(1/\gamma^2), \quad \omega^{(\text{MP})} \rightarrow (\mu_H - \mu_L) / 4\pi\gamma.$$

The first order term for $1/\gamma$ of $\eta^{(\text{MP})}$ vanishes for $\lim_{V \rightarrow \infty} \Delta n^{(1)}(V) = 0$. Thus, under the limit of large dissipation $\gamma \rightarrow \infty$, there is $\eta^{(\text{MP})} \rightarrow 1/2$ to the first order of $1/\gamma$.